http://dx.doi.org/10.5012/bkcs.2014.35.2.651

Assembly and Catalytic Properties of a 3D (4,6)-connected Cobalt-organic Framework with fsh Topology

Chun-lun Ming, Hao Zhang, Guang-yue Li, and Guang-hua Cui*

College of Chemical Engineering, Hebei United University, 46 West Xinhua Road, Tangshan 063009, Hebei P.R. China
**E-mail: tscghua@126.com*
Received November 2, 2013, Accepted November 25, 2013

Key Words : Catalytic property, Cobalt-organic framework, Crystal structure, **fsh** topology

During the past two decades, the construction of novel functional coordination polymers (CPs) has become one of the most intense areas for the sake of inosculating the aesthetic features of intriguing crystalline materials with diverse structural topologies and potential applications in areas of magnetism, adsorption, separation, catalysis, luminescence, and so on.[1-7] Choosing well-designed organic ligands containing modifiable backbones is the key step and the most effective and facile method to build novel CPs. Therefore, significant interest has arisen in the structural tuning of coordination polymers *via* rational selection of with N and/or O-donors as coordination sites in the construction of crystalline materials with the three-dimensional (3D) CPs, such as **pcu**, **msw**, **mok**, **dia**, **srs**, **cds**, **rtl**, *etc*.[8-18] However, there is an unfavorable lack of research about the higher-dimensional networks with the mixed nodes, such as (3,6)-, (4,6)-, (4,8)-, (4,10)-, and (4,12)-connected networks, which are considered to be much more difficult to obtain these networks.[19,20]

The bridging ligand 1,2,4,5-benzenetetracarboxylic acid (H_4btec) has various coordination modes to the metal centers and links metal ions to construct metal-carboxylate frameworks which can be further elevated through the incorporation of bridging flexible two-connector *N*-containing ligands. Herein, we anticipate 1,1-(1,4-butanediyl)bis-1H-benzimidazole (bbbm) ligand, which possesses a favorable *N*-ligating donor for metal ions and a more flexible coordination fashion due to the existence of *cis*- or *trans*- configuration resulting from the free rotation of the benzimidazole rings. In continuation of our exploratory research toward developing a new example of 3D CPs with the mixed nodes based on $btec^{4-}$ ligand, we have been successfully synthesized and structurally characterized a new 3D cobalt(II) coordination polymer $[Co(btec)_{0.5}(bbbm)_{0.5}]_n$. which exhibits a rare binodal 4,6-connected **fsh** net. To the best of our knowledge, only two CPs with this topology (one noninterpenetrating[21] and one interpenetrating **fsh** net[22]) have been reported lately, and the structure of the complex presented here is the first cobalt(II) complex with **fsh** network. Furthermore, the complex as a heterogeneous catalyst for degrading congo red and the fluorescence property have been investigated.

Experimental Section

Materials and Characterization Methods. All the reagents and solvents for synthesis were commercially available and used as received except for bbbm, which was synthesized according to the literature.[23] The elemental analyses (C, H, and N) were performed on a Perkin-Elmer 240C analyzer. Thermal analysis was performed on a Netzsch TG 209 thermal analyzer from room temperature to 800 °C under N_2 at a heating rate of 10 °C/min. FT-IR spectrum was recorded from KBr pellets in the range of 4000-400 cm^{-1} on an Avatar 360 (Nicolet) spectrophotometer. The luminescence spectra for the powdered solid samples were measured at room temperature on a Hitachi F-4500 fluorescence spectrophotometer. The X-ray powder diffraction (XRPD) pattern was recorded on a Rigaku D/Max-2500 diffractometer at 40 kV, 100 mA for a Cu-target tube and a graphite monochromator.

Synthesis of $[Co(btec)_{0.5}(bbbm)_{0.5}]_n$. A mixture of $Co(OAc)_2$ (0.1 mmol, 17.7 mg), bbbm (0.1 mmol, 29.0 mg), H_4btec (0.1 mmol, 25.0 mg), and NaOH (0.4 mmol, 16.0 mg) in 15 mL of distilled H_2O was sealed in a 25 mL Teflon-lined stainless steel container and heated at 140 °C for 3 days. After the mixture cooled to room temperature at a rate of 5 °C/h, pink crystals of the complex were obtained with a yield of 46% (based on Co). Anal. Calcd for $C_{14}H_{10}CoN_2O_4$ (%): C, 51.06; H, 3.06; N, 8.51%. Found: C, 51.12; H, 3.18; N, 8.62%. IR (KBr, cm^{-1}): 3434m, 3136w, 2985w, 1743m, 1607s, 1571s, 1420m, 1373s, 1324w, 1289w, 1221w, 1131w, 919m, 822m, 759m, 581w.

Crystallography. The crystal data for title complex was collected on a Bruker Smart 1000 CCD diffractometer with Mo-Kα radiation (λ = 0.71073 Å) and ω-2θ scan mode at 293 K. A semi-empirical absorption correction was applied using the SADABS program.[24] The structure was solved by direct methods and refined on F^2 by full-matrix least-squares technique using the SHELXL-97 program package.[25] All non-hydrogen atoms were located in difference Fourier maps and refined anisotropically. The H-atoms of organic ligands were generated theoretically onto the specific atoms and refined isotropically. CCDC-967936 contains the supplementary crystallographic data. The crystallographic data is summarized in Table S1 (Supporting Information), and the selected

bond lengths and angles are listed in Table S2 for the complex.

Catalytic Experiment. The complex was used as heterogeneous catalyst (20 mg) for the degradation of the thermostatted dye (congo red solution 50 mL with 20 mg/L), and H_2O_2 (0.5 mL, 30%, w/w) in the aqueous solution. At preset time intervals, samples were taken by a glass syringe and filtered through 0.45 μm membrane filter. The dye concentrations of congo red was measured using a TU-1901 UV-vis spectrophotometer at λ_{max} = 496 nm. The degradation efficiency of congo red was represented as follows:[26]

$$\text{Degradation efficiency} = \frac{(C_0 - C_t)}{C_0} \times 100\% \qquad (1)$$

Where C_0 (mg/L) is the initial concentration of congo red, and C_t (mg/L) is the concentration of congo red remaining in solution, t (min).

Results and Discussion

Single-crystal X-ray diffraction analysis reveals that the complex crystallizes in the triclinic $P\bar{1}$ space group. The asymmetric unit consists of one crystallographically distinguishing Co(II) cation, a half btec^{4-} anion, and a half bbbm ligand. As shown in Figure 1(a), each Co(II) atom exhibits a distorted octahedral environment, the equatorial plane of which comprises four carboxylate oxygen (O1A, O2, O3, O4, A = $-x+2$, $-y$, $-z+2$) atoms from three distinct btec^{4-} anions, one nitrogen atom (N1) belonging to the bbbm ligand and one carboxylate oxygen (O4B, B = $-x+1$, $-y$, $-z+2$) of btec^{4-} inhabiting the apical site. The Co–N bond distance is 2.053(1) Å and the Co–O bond lengths are in the range of 2.027(1)–2.273(1) Å, which are in the normal range of those observed in cobalt complexes.[27]

Each fully deprotonated btec^{4-} bridge acts as a μ_6-bridge linking six cobalt centers, in which two carboxylate groups adopt a μ_2-η^1:η^1-bis-monodentate coordination mode, while the other two carboxylate groups reveal a μ_2-η^2:η^1-chelating coordination mode connecting two Co(II) atoms, respectively (Figure 1(b)). Two Co atoms are bridged by two carboxylate groups to form a $[Co_2(btec)_2]^{4-}$ unit with a Co–Co distance of 8.3129 Å. Such resulting binuclear units make up infinite $[Co_2(btec)_2]_n^{4-}$ 2D slightly distorted brick wall architecture (Figure 1(c)). Furthermore, the bbbm adopts a bis-monodetate fashion coordinating to the Co centers in the *trans*-configuration and the two benzimidazole rings of one bbbm ligand are parallel to each other. To know more about the network, the topology provides a convenient tool in self-assembling and understanding the complicated crystal structures of coordination polymers. Such structures can usually be reduced to simple topological networks with different connectivity of the components. As can be seen Figure 1(d), the flexible bbbm ligands link the adjacent layers to feature a 3D noninterpenetrating network. Thus, the 3D structure of the complex can be simplified as a unique mixed nodes, 4,6-connected **fsh** network with the topology notation of $(4^3.6^3)_2(4^6.6^6.8^3)$ analyzed by TOPOS 4.0 program.[28] In the

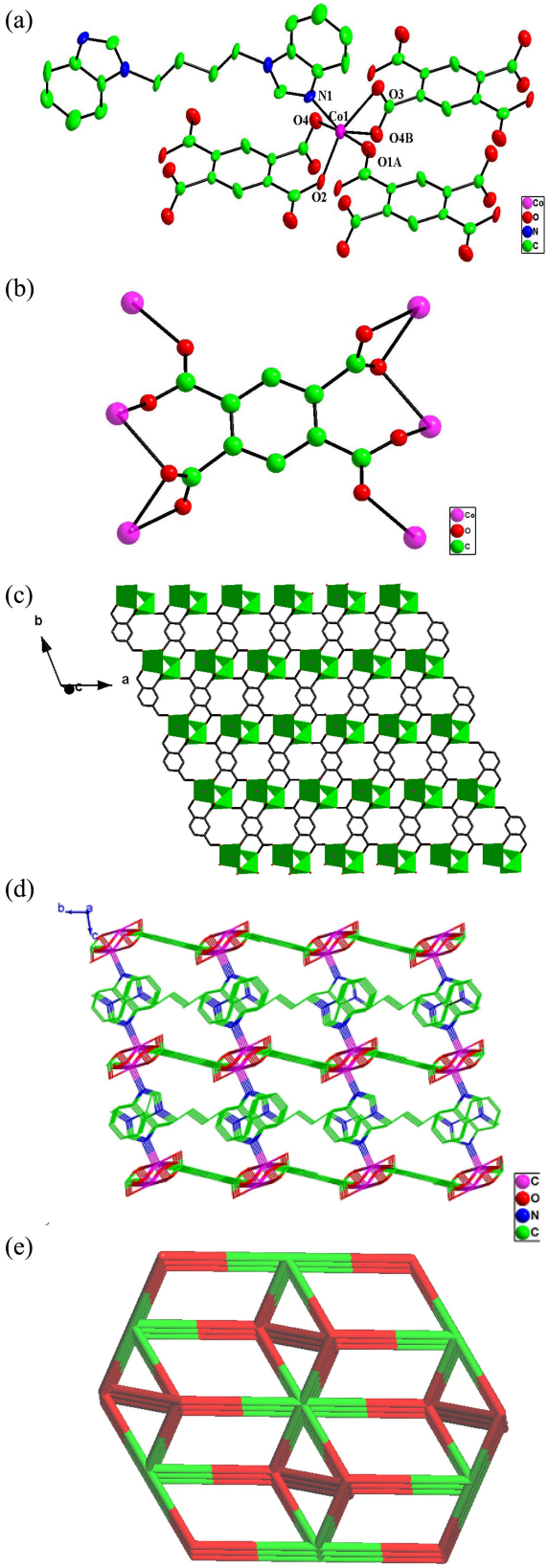

Figure 1. (a) Local coordination geometry of the central Co(II) cation in the complex (all H atoms are omitted for clarity). (b) Coordination mode of the H_4btec ligand in the complex. (c) 2D slightly distorted brick wall architecture consisting of infinite $[Co_2(btec)_2]^{4-}$. (d) Perspective view of the 3D framework. (e) 3D framework with binodal (4,6)-connected **fsh** topology.

topological network, bbbm ligand can be simplified to be linear connectors; each btec^{4-} ligand can be viewed as 6-connected node, which is linked with six Co atoms; each Co center bridges one bbbm and three distinct btec^{4-} ligands, viewed as 4-connected nodes in tetrahedral sphere (Figure 1(e)).

IR Spectrum and XRPD Pattern. The main features in the IR spectrum of the complex concern the carboxylates and *N*-containing benzimidazole ligands. There is no absorption peak between 1730 and 1649 cm^{-1}, indicating that all carboxyl groups of the organic moieties are deprotonated.[29] The strong bands at around 1571 cm^{-1} can be attributed to the $\nu_{(C=N)}$ absorption of the benzimidazole rings. The weak absorption peaks of -CH_2- groups in the complexes appear at around 2985 cm^{-1}. The characteristic peaks of the carboxyl groups appear at *ca*. 1607 cm^{-1} for asymmetric vibrations and at 1373 cm^{-1} for symmetric vibrations in the complex.

The simulated and experimental XRPD patterns of compound, obtained at room temperature, are shown in Figure S1. Their peak positions are in good consistency with each other, indicating the phase purity of the as-synthesized samples.

Thermal Analysis. The thermogravimetric analysis of powder sample of the complex was carried out from 18 to 800 °C under a nitrogen atmosphere at a heating rate of 10 °C min^{-1}, as shown in Figure S2. The TGA curve for the compound shows that chemical decomposition starts at 448 °C and ends at 595 °C with the weight loss of 77.10%, equivalent to the removal of coordinated bbbm and 1,2,4,5-benzenetetracarboxylate ligands (calcd. 77.24%); the remaining weight corresponds to CoO.

Fluminescence Property. Luminescent metal-organic frameworks have received remarkable attention owing to their higher thermal stability than the pure organic ligand and the ability to affect the emission wavelength and intensity of the organic material by metal coordination.

The emission spectra of complex along with the free bbbm ligand have been investigated in the solid state at room temperature. The emission peaks are shown in Figure 3. The maximum of emission band is at about 400 nm (λ_{ex} = 323 nm) for the bbbm ligand, which may be ascribed to the $\pi \rightarrow \pi^*$ electronic transition of the bbbm.[30] Comparing with the free bbbm ligand, the emission maximum of the complex (λ_{em} = 355 nm, λ_{ex} = 290 nm) undergoes blue-shifted 45 nm, which could be derived from the reduced conjugation of the bbbm ligand upon coordination. The emission band of the complex can be tentatively attributed to the intraligand charge transfer transitions.[31]

Catalytic Degradation Experiment. Although CPs still cannot completely replace inorganic materials, such as the classical molecular sieves and zeolites in catalysis, CPs can be regarded as the good candidates for fine organic synthesis and enantioselective catalysis under mild conditions. Generally, the CPs catalytic activity may originate from the open metal sites, reactive functional groups and host matrices or nano-metric reaction cavities.[32] Congo red (sodium salt of benzidinediazo-bis-1-naphtylamine-4 sulfonic acid) is one of the important azo dyes, used for textiles, printing and dyeing, paper, rubber, plastics industries, etc. Due to its structural stability, congo red is difficult to biodegrade. Recently, much attention has been focused on the heterogeneous Fenton and Fenton-like reactions to oxidize contaminants of concern such as azo dyes, which largely depend on transition metal-based catalysts.[33] Moreover, hydrogen peroxide (H_2O_2) is a precursor of hydroxyl radicals, which can degrade and mineralization azo dye molecules in water.[34]

The degradation experiments of congo red by hydrogen peroxide activated with the complex were investigated. As shown in Figure 4, in the control experiment, the dye and H_2O_2 mixture is stable without any distinct change in the absorbance of dye, which indicates that there is no reaction takes place between the dye and H_2O_2, and the degradation efficiency was very low with only 9.70 % after 110 min. The reaction system is setup by adding the catalyst and H_2O_2 into the dye solution. Addition of 20 mg catalyst in the reaction system, the rate of the catalytic reaction increases quickly in first 10 min (up to 81.00%), then the congo red oxidation proceeded in a gradual manner, in which degradation efficiencies were up to 99.11% after 110 min, indicating the complex is a highly active for the Fenton-like reaction to decompose congo red. Compared with the similar catalyst, the Complex has a remarkable performance on degradation of congo red.[35]

Based on the experimental observations, the mode of action of the catalysis was suggested utilizing the redox properties of H_2O_2 in Fenton process.[36]

The Fenton's reagent involves reaction of Co(II) ion with hydrogen peroxide to produce hydroxyl radicals, which are strong oxidizing reagents that react with the dye solution (congo red) causing its degradation.

$$H_2O_2 + \text{Co(II)-MOF} \rightarrow \cdot OH + OH^- + \text{Co(III)-MOF}$$
$$H_2O_2 + \text{Co(III)-MOF} \rightarrow \text{Co(II)-MOF} + \cdot OOH + H^+$$
$$\text{Azo dye} + \cdot OH \rightarrow \text{oxidation products}$$

The hydroxyl radical propagates the reaction by reacting with CR dye to produce further radicals, which can then

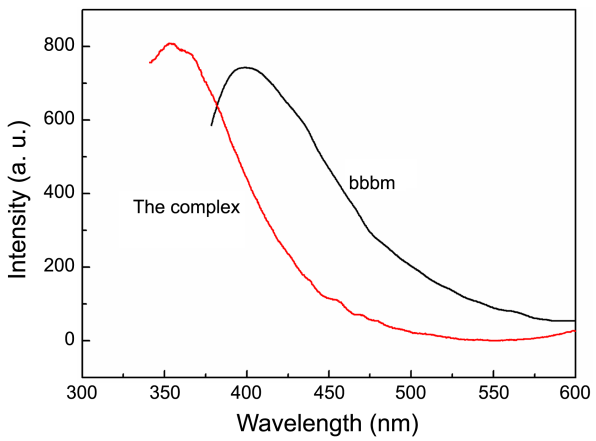

Figure 2. The emission spectra of the complex and the free bbbm ligand.

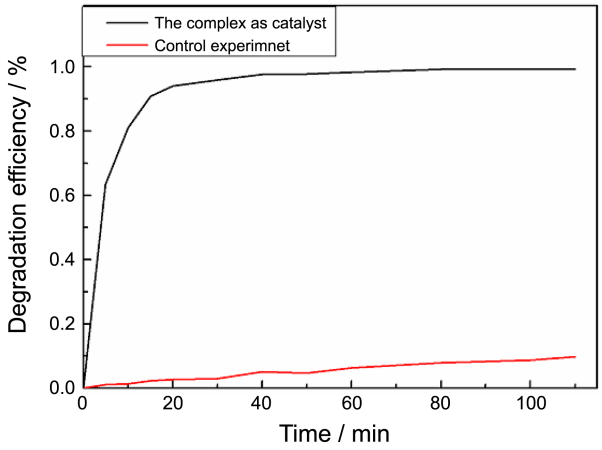

Figure 3. Kinetic profile for catalytic degradation of congo red with H_2O_2 in the presence of heterogeneous catalyst: the black line reveals the degradation efficiency with catalyst, the red line represents the degradation efficiency without catalyst.

react in many different steps.

$$\cdot OH + CR \rightarrow \cdot CR + H_2O$$
$$\cdot CR + H_2O_2 \rightarrow CR\text{-}OH + \cdot OH$$

In summary, we have synthesized and topologically characterized a cobalt(II) metal-organic framework with a unique (4,6)-connected **fsh** topology. Furthermore, the complex displays the high catalytic activity on Fenton-like process to degrade congo red azo dye.

Supplementary Material. CCDC number: 967936 for the complex. The data can be obtained free of charge *via* https://services.ccdc.cam.ac.uk/structure_deposit (or from the Cambridge Cryst allographic Data Centre, 12, Union Road, Cambridge CB21EZ, UK; fax: (44)1223-336-033(44); or deposit@ccdc .cam.ac.uk).

Acknowledgments. Financial support from the National Natural Science Foundation of China (Nos. 11247281), and Excellent Youth Fund of Hebei Province Department of Education (Y2012010). And the publication cost of this paper was supported by the Korean Chemical Society.

References

1. Furukawa, H.; Cordova, K. E.; O'Keeffe, M.; Yaghi, Omar, M. *Science* **2013**, *341*, 1230444.
2. Ma, Z. B.; Moulton, B. *Coord. Chem. Rev.* **2011**, *255*, 1623.
3. Xu, W. J.; Zhang, L. Y.; Tang, J, N.; Wang, D. Y.; Pan, G. H.; Fang, Y. *Bull. Korean Chem. Soc.* **2013**, *34*, 2375.
4. Lin, Z. J.; Tong, M. L. *Coord. Chem. Rev.* **2011**, *255*, 421.
5. Chen, S. S.; Zhao, Y.; Fan, J.; Okamura, T. A.; Bai, Z. S.; Chen, Z. H.; Sun, W. Y. *CrystEngComm*. **2012**, *14*, 3564.
6. Xia, C. K.; Lu, C. Z.; Yuan, D. Q.; Zhang, Q. Z.; Wu, X. Y.; Xiang, S. C.; Zhang, J. J.; Wu, D. M. *CrystEngComm*. **2006**, *8*, 281.
7. Du, M.; Li, C. P.; Liu, C. S.; Fang, S. M. *Coord. Chem. Rev.* **2013**, *257*, 1282.
8. Li, Y. W.; Ma, H.; Chen, Y. Q.; He, K. H.; Li, Z. X.; Bu, X. H. *Cryst. Growth Des*. **2012**, *12*, 189.
9. Li, Z. X.; Xu, Y.; Zuo, Y.; Li, L.; Pan, Q. H.; Hu, T. L.; Bu, X. H. *Cryst. Growth Des*. **2009**, *9*, 3904.
10. Rao, C. N. R.; Natarajan, S.; Vaidhyanathan, R. *Angew. Chem. Int. Ed*. **2004**, *43*, 1466.
11. Qin, L.; Zheng, J.; Xiao, S. L.; Zheng, X. H.; Cui, G. H. *Inorg. Chem. Commun*. **2013**, *34*, 71.
12. Xiao, S. L.; Cui, G. H.; Blatov, V. B.; Geng, J. C.; Li, G. Y. *Bull. Korean Chem. Soc.* **2013**, *34*, 1891.
13. Sumida, K.; Rogow, D. L.; Mason, J. A.; McDonald, T. M.; Bloch, E. D.; Herm, Z. R.; Bae, T. H.; Long, J. R. *Chem. Rev.* **2012**, *112*, 724.
14. Wang, X. W.; Chen, J. Z.; Liu, J. H. *Cryst. Growth Des*. **2007**, *7*, 1227.
15. Han, L.; Zhou, Y. *Inorg. Chem. Commun*. **2008**, *11*, 385.
16. Qin, Y. L.; Liu, J.; Hou, J. J.; Yao, R. X.; Zhang, X. M. *Cryst. Growth Des*. **2012**, *12*, 6068.
17. Bisht, K. K.; Suresh, E. *Cryst. Growth Des*. **2013**, *13*, 664.
18. Zhou, Y.; Han, L.; Pan, J. G.; Li, X.; Zheng, Y. Q. *Inorg. Chem. Commun*. **2008**, *11*, 1107.
19. He, C. H.; Jiao, C. H.; Geng, J. C.; Cui, G. H. *J. Coord. Chem*. **2012**, *65*, 2294.
20. Geng, J. C.; Qin, L.; Du, X.; Xiao, S. L.; Cui, G. H. *Z. Anorg. Allg. Chem*. **2012**, *638*, 1233.
21. Yang, G. P.; Hou, L.; Wang, Y. Y.; Zhang, Y. N.; Shi, Q. Z.; Batten, S. R. *Cryst. Growth Des*. **2011**, *11*, 936.
22. Guo, F.; Wang, F.; Yang, H.; Zhang, X. L.; Zhang, J. *Inorg. Chem*. **2012**, *51*, 9677.
23. Xie, X. J.; Yang, G. S.; Cheng, L.; Wang, F. *Huaxue Shiji (Chin. Ed.)* **2000**, *22*, 222.
24. Sheldrick, G. M.; SADABS (version 2.03), *Program for Empirical Absorption Correction of Area Detector Data*, University of Göttingen, Göttingen (Germany) 1996.
25. Sheldrick, G. M. *Acta Crystallogr.* **2008**, *A64*, 112.
26. Fan, J.; Guo, Y. H.; Wang, J. J.; Fan, M. H. *J. Hazard. Mater.* **2009**, *166*, 904.
27. Liu, G. C.; Y, S.; Wang, X. L.; Lin, H. Y.; Tian, A. X.; Zhang, J. W. *Russ. J. Coord. Chem*. **2009**, *35*, 25.
28. Blatov, V. A. *Struct. Chem*. **2012**, *23*, 955.
29. Tao, B.; Lei, W.; Cheng, F. R.; Xia, H. *Bull. Korean Chem. Soc.* **2012**, *33*, 1929.
30. Bai, H. Y.; Wang, S. M.; Fan, W. Q.; Liu, C. B.; Che, G. B. *Polyhedron*. **2013**, *50*, 193.
31. Jin, S. W.; Wang, D. Q.; Chen, W. Z. *Inorg. Chem. Commun*. **2007**, *10*, 685.
32. Isaeva, V. I.; Kustov, L. M. *Petrol. Chem*. **2010**, *50*, 167.
33. Mane, V. S.; Vijay Babu, P. V. *J. Taiwan. Inst. Chem. Eng*. **2013**, *44*, 81.
34. Ramirez, J. H.; Duarte, F. M.; Martins, F. G.; Costa, C. A.; Madeira, L. M. *Chem. Eng. J*. **2009**, *148*, 394.
35. Etaiw, S. E. H.; Badr El-din, A. S.; El-bendary, M. M. *Z. Anorg. Allg. Chem*. **2013**, *639*, 810.
36. Schrank, S. G.; Santos, J. N. R.; Souza, D. S.; Souza, E. E. S. *J. Photochem. Photobiol., A* **2007**, *186*, 125.